



iJRASET

International Journal For Research in
Applied Science and Engineering Technology



INTERNATIONAL JOURNAL FOR RESEARCH

IN APPLIED SCIENCE & ENGINEERING TECHNOLOGY

Volume: 3

Issue: III

Month of publication: March 2015

DOI:

www.ijraset.com

Call: ☎ 08813907089

E-mail ID: ijraset@gmail.com

Kinetics, Thermodynamics and Mass Transfer Studies on Application of Titania Nanofibers for Heavy Metal Adsorption

Abhilasha Dixit^{#1}, P.K.Mishra^{*2}, M.S.Alam^{#3}

[#]Motilal Nehru National Institute of Technology, Allahabad, India-211004

^{*}Indian Institute of Technology (BHU), Varanasi, India-221005

Abstract— In the present work, lab synthesized TiO_2 nano-adsorbents in fiber form with surface area of about $740 \text{ m}^2/\text{g}$ and promising FTIR results were employed for the removal of Pb(II) and Zn(II) ions from aqueous solutions by batch-adsorption technique. The SEM results indicated well aligned fibers with average diameter of 255 nm . The effect of contact time, initial concentration of metal ions, temperature, solution pH and adsorbent dose on the amount of metal ions adsorbed was investigated. The adsorption process was fast for both the metals, and equilibrium was achieved within 120 min. The amount of metals adsorbed increased as temperature increased, suggesting an endothermic adsorption. The process followed second order kinetics and the data gave best fit for Langmuir isotherm. The Mass transfer mechanism appeared to be film diffusion controlled and the thermodynamic parameters ΔG° , ΔH° and ΔS° highlighted the fact that the adsorption was spontaneous and endothermic in nature.

Keywords— Nano, adsorption, heavy metal, kinetics, thermodynamics, mass transfer

I. INTRODUCTION

Over the last three decades there has been an increase in global concern over public health impacts attributed to environmental pollution, in particular, the non biodegradable and highly toxic heavy metals. The pollutants flux increase is directly related to the increase in anthropogenic activities. The dispersion of metals in the atmosphere results in their mobilization. It is important for this reason to study the process that limits its release, and also to evaluate the effectiveness of the processes employed to treat industrial effluents. Lead and Zinc are amongst heavy metals entering the environment majorly via e-waste. Also the extensive use of lead antiknock additives in gasoline has made lead perhaps the most widely distributed toxic heavy metal in the urban environment. Lead can damage the fetal brain and hit diseases of the kidneys, circulatory system, and nervous system and Zinc causes depression, lethargy, neurological signs and increased thirst [1]. Zinc is present in many alloys and is also found in a number of pharmaceutical samples and in airborne particulates, causing environmental pollution.

Chemical precipitation [2], ion exchange process [3,4], electrolytic methods [5], organic-based ligand precipitation [6], membrane and reverse osmosis processes [7] have been used to remove metal ions from wastewater effluents. These methods score low because of the high capital and operating costs and/or the ineffectiveness in meeting stringent effluent standards. Adsorption technology has gained a wider application due to its inherent low cost, simplicity, versatility and robustness [8].

Metal oxides are effective heavy metal adsorbents since they provide high adsorption capacity, rapid adsorption rate and simple separation. Nanostructured metal oxide materials have attracted considerable attention because of their potential applications in many areas such as electronics, photonics, sensors and catalysis [9-14]. Nanosized ceramics with large surface area per unit mass can have enhanced electrical, physical, and chemical properties with respect to their bulk counterparts [15,16]. Among all metal oxides at nanoscale, TiO_2 possess high potential for environmental applications due to its physical and chemical stability, relatively lower cost, non-toxicity, resistance to corrosion, and large surface area, and stable colloidal suspension [17-19]. Various morphological advancements in TiO_2 at nanoscale are being tried out by scientists worldwide, fibers being one promising form of it. Various approaches for the preparation of nano- and micro-structures of titania have been reported, such as sol-gel processes, pyrolysis, electrospinning, chemical vapor deposition and hydrothermal methods [20-24].

The present work reports the effectiveness of lab synthesized electrospun Titania nanofibers in Pb and Zn adsorption from aqueous solutions with emphasis on kinetic, thermodynamic and mass transfer behavior.

II. MATERIAL AND METHODS

Titania nanofiber synthesis via combined sol-gel and electrospinning processes was adapted from Dan Li and Younan Xia [25] wherein a polymer based sol-gel solution containing TTIP (97%), acetic acid and ethanol in the ratio 1:2:2 (obtained from Merck) was electrospun onto a collector plate. A constant feed rate of 1 mL/h was maintained by the syringe pump to ensure

International Journal for Research in Applied Science & Engineering Technology (IJRASET)

the steady deposition of nanofibers on the collector plate. The obtained fibers were kept in air for 5 hours for complete hydrolysis. These fibers were then calcined at 500°C in muffle furnace for 3 hours in order to eliminate the organic components and to obtain the crystalline structure of fibers.

The stock solutions of Pb(II) and Zn(II) were prepared from $\text{Pb}(\text{NO}_3)_2$ and $\text{Zn}(\text{NO}_3)_2 \cdot 6\text{H}_2\text{O}$ respectively. The solution pH was adjusted with HNO_3 and NaOH solutions. All batch adsorption experiments were performed in 500 mL flasks, containing 100 mL metal solution with shaking at 200 rpm on a rotary shaker for desired duration. The concentration of Pb(II) and Zn(II) in aqueous solution were determined by Atomic Absorption Spectroscopy (Aurora Instruments Ltd, Canada). The metal concentration of a sample was estimated using a calibration curve (absorbance versus concentration) prepared using respective standard concentration metal solutions. Adsorption process was quantified by calculating the sorption percentage (%R) as defined by Eq. 1:

$$\% R = \frac{C_o - C_e}{C_o} \times 100 \quad (1)$$

where C_o is the initial concentration and C_e is the equilibrium concentration (mg/L). The amount of ions adsorbed per unit mass of adsorbent, q_e (mg/g) is evaluated using Eq. 2:

$$q_e = \frac{C_o - C_e}{W} V \quad (2)$$

where C_o and C_e (mg/L) as in Eq. (1), V (mL) is the volume of metal solution, and W (mg) is the weight of adsorbent, TNF in this case.

The effects of different experimental parameters such as pH (3, 5, 7 and 9), adsorbent dosage (0.01 to 0.08 g/100mL), contact time (30 to 180 mins), temperature (25, 30 and 35°C) and initial concentrations of Pb(II) and Zn(II) (5 and 10 mg/L) on the adsorption kinetics were evaluated.

III.RESULTS AND DISCUSSION

A. Adsorbent characterization

Combined sol-gel and electrospinning techniques showed promising results for titania nanofiber synthesis. Fig. 1 represents Scanning Electron Microscopy results. The synthesized fibers appeared well aligned and had smooth morphology. There were not many breakages and the fibers had good continuous length which definitely makes the weaving strong and strengthens the fiber mat as a whole. The average diameter of the fibers came out be around 255nm.

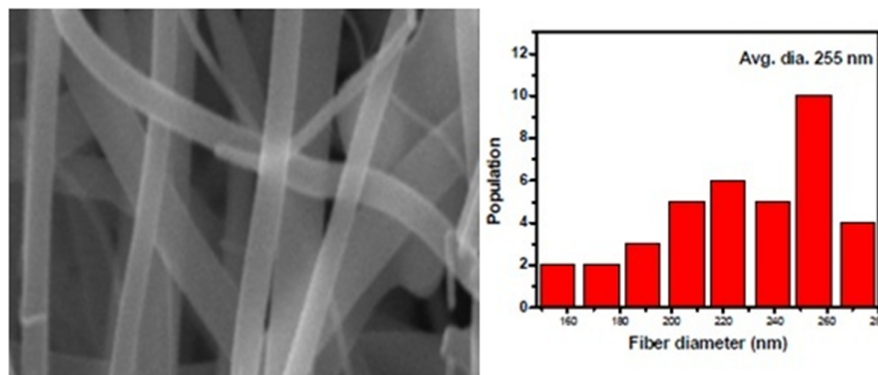


Fig. 1 SEM image and average diameter plot of electrospun Titania nanofiber

The larger the surface area, the better is the adsorption process. The surface area (BET) measurements of the adsorbent was obtained using BET method with nitrogen gas at 77K using Micrometrics surface area analyzer and results were promising. The fiber had surface area as large as 740.188 m²/g.

The spectra of the fiber samples were measured by Fourier transform infrared spectroscopy (FTIR) within the range of 400–4000 cm⁻¹ wave number. Table 1 represents FTIR spectroscopic characteristics. A particular band position has a possible assignment as mentioned in the table. The results indicate promising presence of Ti stretching band. The presence of OH group and physisorbed water is also indicated at their respective band positions.

International Journal for Research in Applied Science & Engineering Technology (IJRASET)

TABLE I
FTIR ANALYSIS

Peak (cm ⁻¹)	Inference
3700 - 3000	OH group
1632	Physisorbed water
900 - 450	Ti-O-Ti stretching

The characterization results indicated that the synthesized titania fiber can be employed as adsorbent for heavy metal uptake from aqueous solutions. Various process parameters known to affect the adsorption process were studied in detail.

B. Effect of paramaters

1) *Effect of pH*: The pH of the system plays a vital role since it influences the protonation or deprotonation. Adsorption experiments for both Pb and Zn were carried out in pH range of 3 – 9, keeping all other parameters constant (Fig. 2). The Pb and Zn uptake at different pH values showed the same trend, the adsorption increased with increasing pH of the solution. The increase in metal removal with increase in pH values can be explained on the basis of a decrease in competition between proton and the metal cations for the same functional groups and by the decrease in positive charge of the adsorbent which results in a lower electrostatic repulsion between the metal cations and the surface. The maximum adsorption rate was observed at the pH value of 5 which was thereafter fixed for all experiments.

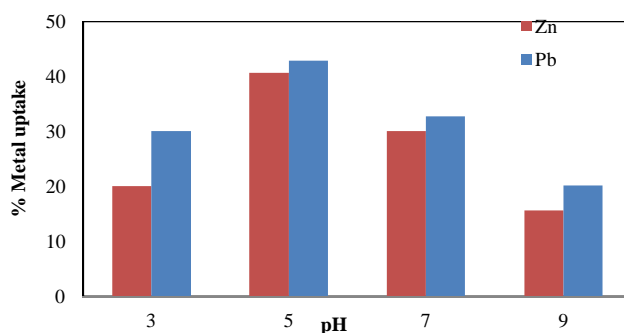


Fig. 2 Effect of pH on metal uptake.

2) *Effect of initial metal ion concentration and contact time*: The uptake of both Pb and Zn at concentrations of 5 and 10 mg/L each was investigated at different times to study the influence of adsorbent-adsorbate contact time on metal uptake. With the increase in contact time, the percent metal uptake was found to increase till 120 min, thereafter no remarkable increase in uptake capacity was observed, i.e after the attainment of equilibrium the removal efficiency remained almost constant. It was observed that metal uptake efficiency of TNF decreased when the metal concentration was increased from 5 mg/L to 10 mg/L as indicated in fig. 3. This might be due to the fact that with an increase in metal ion - adsorbent ratio, the adsorption starts targeting lower energy sites since the higher energy sites are saturated which results in the decreased metal uptake with increase in initial metal concentration [26].

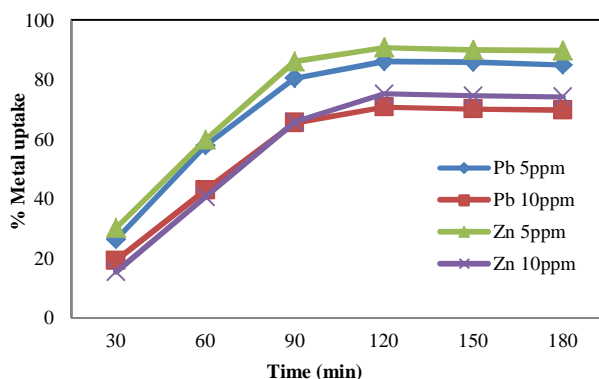


Fig. 3 Effect of contact time and initial metal concentration on Pb and Zn uptake.

International Journal for Research in Applied Science & Engineering Technology (IJRASET)

3) *Effect of adsorbent dose:* The effect of adsorbent dose on metal uptake was studied by varying the dose from 0.01 to 0.08 mg/100mL TNF for both Pb and Zn (5 & 10 mg/L each) (Fig. 4). The metal adsorption appeared to increase initially with increasing adsorbent dose which can be attributed to the availability of greater surface area hence more sites promoting easier and faster adsorption. At an adsorbent dose of 0.05 mg/100mL, the adsorption capacity reaches a stable (maximum) value after which further increase in the adsorbent dose doesn't significantly contribute to the process which might be due to the fact that above a certain dose, the amount of adsorbent ions and free ions remains constant and hence does not affect metal uptake.

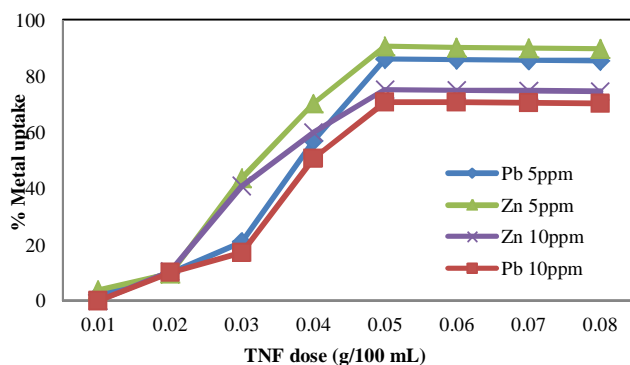


Fig. 4: Effect of adsorbent dose on Pb and Zn uptake.

4) *Effect of Temperature:* The effect of temperature is important in adsorption systems since change in temperature can cause the change in the equilibrium constant and adsorption capacity of the adsorbent, thereby affecting the overall process. To study the effect of temperature on metal uptake, the batch adsorption experiments were carried out at 25°C, 30°C and 35°C and results are plotted in Fig. 5. Maximum metal uptake was observed at a temperature of 30°C. The adsorption percentage of both Pb and Zn was seen to be increasing with increase in temperature from 25°C to 30°C. Further increase in temperature to 35°C decreases the adsorption since the increase in temperature increases the mobility of the adsorbate resulting in decreased adsorption.

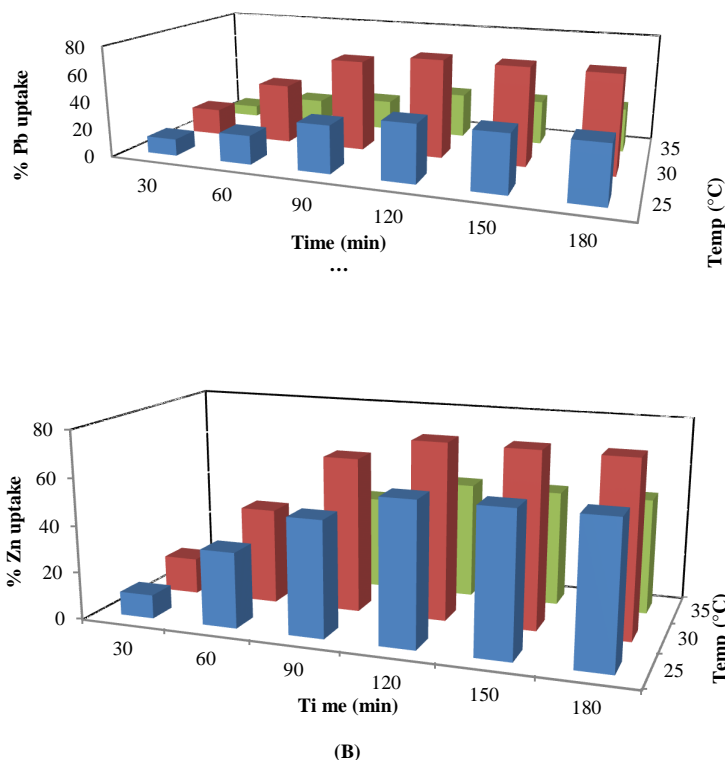


Fig. 5: Effect of temperature on metal uptake (A) Pb(II) (B) Zn(II)

International Journal for Research in Applied Science & Engineering Technology (IJRASET)

C. Adsorption mechanism

1) *Isothermal modeling*: The purpose of the adsorption isotherms is to relate the adsorbate concentration in the bulk and the adsorbed amount at the interface. The equilibrium adsorption isotherm, characterized by certain constants expresses surface properties and the affinity of the adsorbent towards adsorbate, and is important for designing an adsorption system as these models describe the interactive behavior of the solution and the adsorbent. The isotherm results were analyzed using the Langmuir and Freundlich isotherms.

Langmuir and Freundlich isotherms: The Langmuir adsorption model is based on the assumption that maximum adsorption corresponds to a saturated monolayer of solute molecules on the adsorbent surface, with no lateral interaction between the sorbed molecules [27]. Langmuir model assumes the sorbent to be structurally homogeneous. The isotherm data was linearized using the Langmuir equation, expressed as Eq 3 and plotted between C_e/q_e versus C_e as shown in fig. 6A.

$$\frac{C_e}{q_e} = \frac{1}{q_{mb}} + \frac{C_e}{q_m} \quad (3)$$

where q_e is the amount of metal ions sorbed per unit mass of the sorbent (mg/g) and C_e the amount of metal ions in the liquid phase at equilibrium (mg/L), q_m is the maximum adsorption capacity and b is the Langmuir constant. A dimensionless constant, R_L calculated using Eq 4 describes the type of Langmuir isotherm; irreversible ($R_L=0$), favorable ($0 < R_L < 1$) and linear or unfavorable ($R_L > 1$).

$$R_L = \frac{1}{1 + bC_i} \quad (4)$$

The value of q_m (mg/g) which is a measure of the monolayer adsorption capacity of TNF was observed to be 2.381, 2.933 and 2.90, 2.545 for Pb (5 and 10 ppm) and Zn (5 and 10ppm) respectively. The R_L values for both the ions at both concentrations were observed in the range $0 < R_L < 1$ which is an indication of adsorption favorability.

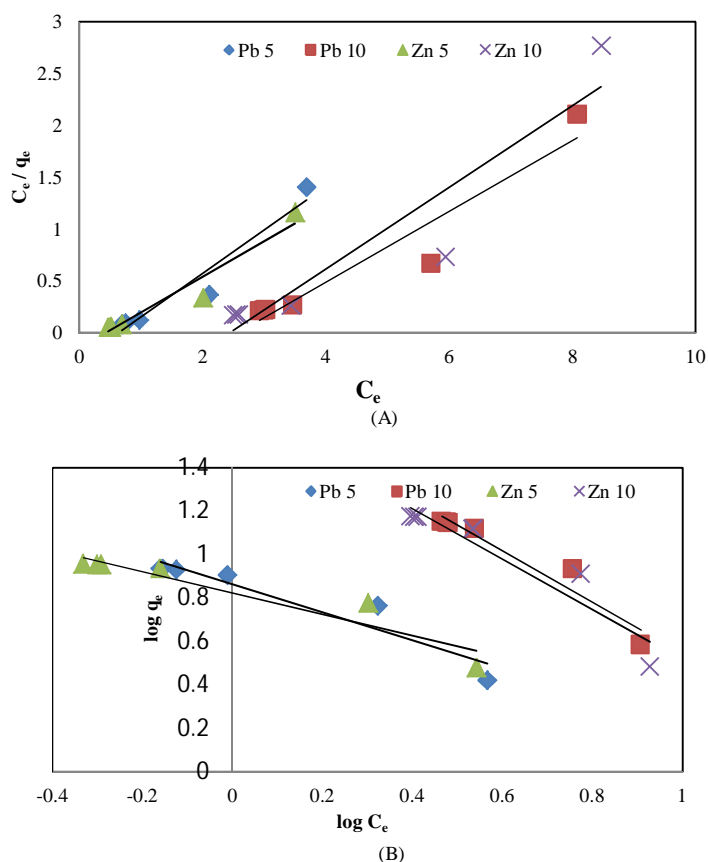


Fig. 6: Isothermal modeling plots for Pb and Zn (A) Langmuir (B) Freundlich

The Freundlich isotherm is an empirical equation employed to describe heterogeneous systems [28]. The Freundlich equation is expressed as:

International Journal for Research in Applied Science & Engineering Technology (IJRASET)

$$q_e = (K_f)(C_e)^{-n} \quad (5)$$

where k_f and n are Freundlich constants with k_f being adsorption capacity of the sorbent and n giving an indication of how favorable the adsorption process is. The values of k_f and n , calculated from the intercept and slope of the plot $\log q_e$ vs $\log C_e$ (fig. 6B), determine the steepness and curvature of the isotherm [29]. The values of $1/n$, less than unity is an indication that significant adsorption takes place at lower concentration but increase in the adsorbed amount with concentration becomes less significant at higher concentration and vice versa [30]. The values of n which is related to the distribution of bonded ions on the adsorbent surface obtained from freundlich plot were - 1.565, - 0.847 and - 2.05, - 0.864 for Pb (5 mg/L, 10 mg/L) and Zn (5 mg/L, 10 mg/L) respectively. Even though the regression values seem fine enough, the negative values of n indicate unfavorable adsorption.

The regression values and the values of constants for both Langmuir and freundlich isotherms are tabulated in table 2. The regression values for both Langmuir and Freundlich plots seem quite close. While comparing the other constant values, the negative n values for freundlich plot was a setback for adsorption favorability.

TABLE III ISOTHERM PARAMETERS FOR METAL ION ADSORPTION

Ion	Concentration (mg/L)	Isotherm					
		Langmuir parameters			Freundlich parameters		
		q_m	R_L	R^2	k_f	n	R^2
Pb	5	2.381	0.428	0.936	0.861	- 1.565	0.899
	10	2.933	0.227	0.917	1.726	- 0.847	0.933
Zn	5	2.90	0.367	0.940	0.823	- 2.05	0.896
	10	2.545	0.203	0.879	1.671	- 0.864	0.9

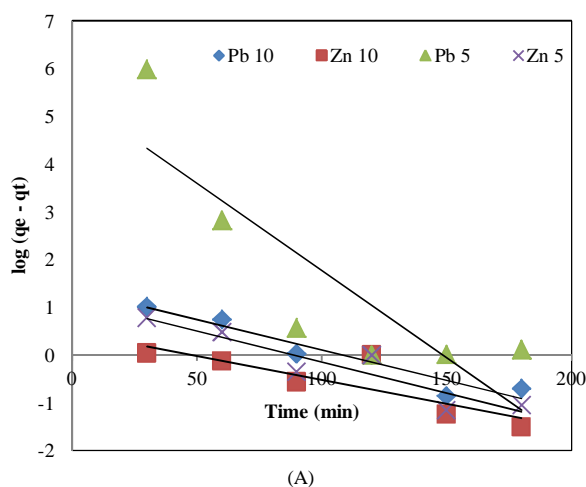
2) *Kinetic modeling*: The adsorption kinetics depicts the rate of adsorbate uptake in terms of surface tension at the solid-liquid interface [31]. Determination of rate controlling mechanism by studying kinetic models can give an idea of the mechanism involved.

Pseudo first and second order kinetics

The experimental data were tried for Pseudo-first order kinetic model represented by Lagergren equation given as Eq. 6 [32]:

$$\log(q_e - q_t) = \log q_e - \frac{k_1 t}{2.303} \quad (6)$$

where q_e and q_t (mg/g) are the amounts of metal ions adsorbed onto TNF at equilibrium and at time t and k_1 (min^{-1}) is the rate constant. Plot of $\log (q_e - q_t)$ vs t (fig. 7A), gives the values of k_1 and q_e . While the constant values were fine, the regression value did not appear very impressive.



International Journal for Research in Applied Science & Engineering Technology (IJRASET)

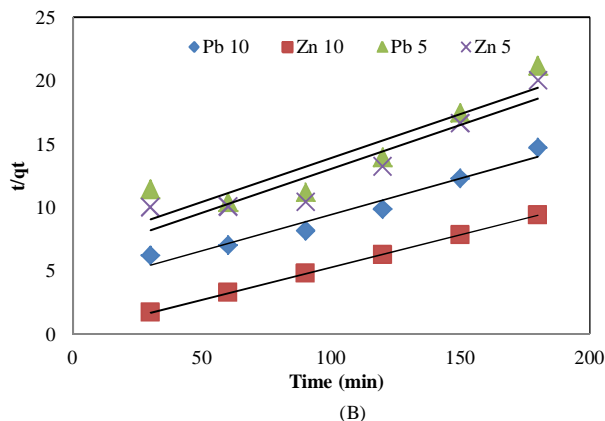


Fig. 7: Kinetic modeling (A) Pseudo first order (B) Pseudo second order

Pseudo-second-order equation stands for chemisorption and can be expressed as Eq. 7 [33]:

$$\frac{t}{qt} = \frac{1}{k_2 q_e^2} + \frac{t}{q_e} \quad (7)$$

where k_2 (g/mmol min) is the adsorption rate constant of pseudo second-order reaction. The plots of t/qt vs. t (fig.7B) gave rate parameters.

Table 3 enlists pseudo first and second order parameters as obtained from the graphs. The regression values for second order were high for both Pb and Zn. Also the constant values were better for second order than first order.

TABLE III
PSEUDO FIRST AND SECOND ORDER RATE PARAMETERS

Ions	Concentration (mg/L)	Pseudo first order			Pseudo second order		
		k_1	q_e	R^2	k_2	q_e	R^2
Pb	5	0.083	2.267	0.722	6.965	2.69	0.933
	10	0.028	3.975	0.917	3.686	5.7	0.96
Zn	5	0.30	3.187	0.86	6.081	2.82	0.976
	10	0.023	1.632	0.712	0.133	5.1	0.99

3) *Mass Transfer Mechanism*: Diffusion occurs by virtue of concentration gradient and rate of sorbate transport is influenced by its interaction with the sorbent. Intraparticle diffusion, a transport process involving movement of species from the bulk of the solution to the solid phase describes the adsorption process occurring on a porous adsorbent. To determine the rate-limiting step of the overall adsorption process, the following models were analyzed:

Weber and Morris model

Weber and Morris Intraparticle diffusion model represented by Eq.8 is a plot of the amount of sorbate adsorbed, q_t (mg/g) and the square root of the time which gives the rate constant.

$$q_t = k_i (\sqrt{t}) \quad (8)$$

where, k_i intraparticle diffusion constant. The experimental data for Pb and Zn adsorption is plotted in fig. 8A. Both the metals follow almost the same graph trend.

The graph trend in fig. 8A represents three different phases. The first part follows a linear trend which corresponds to the fast uptake of sorbate, followed by a stage where sorbate uptake speeds up reflecting non consecutive diffusion of sorbate molecules into the larger pores within the sorbent and finally the third and the last phase where, diffusion remains fairly constant due to pore volume being exhausted. The values of k_i for Pb adsorption came out to be 0.743 and 1.311 for 5 mg/L and 10 mg/L respectively whereas for Zn, k_i values were found to be 0.761 and 1.554 for 5 mg/L and 10 mg/L respectively. It can be seen that the adsorbate concentration does not affect the diffusion pattern. The uptake mechanism assumes intraparticle diffusion only if the following conditions are met for the plot q_t vs $t^{1/2}$:

- High R^2 values to ascertain applicability and,
- Straight line passing through the origin

A deviation from the above shows that the mode of transport is affected by more than one process [34]. This gives an

International Journal for Research in Applied Science & Engineering Technology (IJRASET)

indication that intraparticle diffusion is not only the rate limiting step and there might be a possibility of some degree of film diffusion control. The rate of uptake is limited by the size of adsorbate molecule, the adsorbate concentration and its affinity towards the adsorbent, the diffusion coefficient of the adsorbate in the bulk, the adsorbent pore size distribution and the degree of mixing [35].

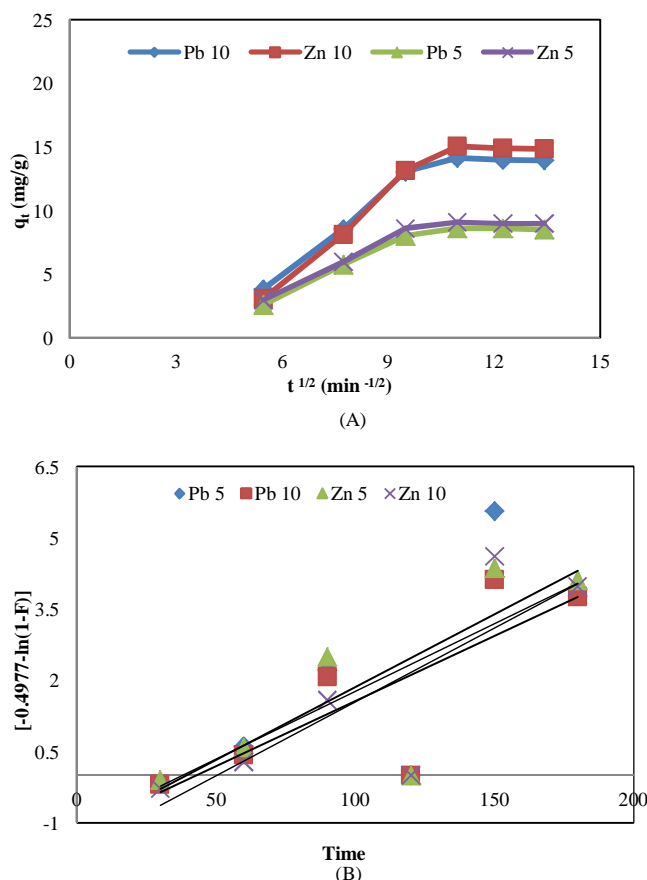


Fig. 8: Mass transfer plots for Pb and Zn adsorption on TNF with varying concentrations at different times (A) Weber and Morris (B) Boyd plot

Boyd model

The contribution of film diffusion is often confirmed using the model given by Boyd, as represented by Eq.9 [36]:

$$F = 1 - \frac{6}{\pi^2} \sum_{n=1}^{\infty} \frac{1}{n^2} \exp(-n^2 Bt) \quad (9)$$

which can be rewritten as,

$$Bt = [-0.4977 - \ln(1 - F)] \quad (10)$$

where, F is the fractional attainment of equilibrium at any time t and B is the time constant. The experimental values can be plotted as $[-0.4977 - \ln(1-F)]$ against time to test its linearity as shown in fig.8B. If the plot is in the form of straight line passing through the origin, this indicates that sorption processes are governed by particle-diffusion mechanisms; otherwise, they are controlled by film diffusion [37]. Figure indicates that the plots were neither linear nor passed through the origin for both Pb and Zn suggesting the film diffusion-controlled mechanism.

4) *Thermodynamic parameters:* Thermodynamic parameters such as free energy change (ΔG°), enthalpy change (ΔH°) and entropy change (ΔS°) were calculated from the variations of the thermodynamic distribution coefficient, K with change in temperature according to the following equations:

$$\Delta G^\circ = RT \ln K \quad (11)$$

$$\Delta G^\circ = \Delta H^\circ - T(\Delta S^\circ) \quad (12)$$

Table 4 gives the values for the thermodynamic parameters. It can be marked that the ΔH° values are all positive for both Pb and Zn which indicates the endothermic nature of the adsorption process. The negative values of ΔG° and ΔS° represent the

International Journal for Research in Applied Science & Engineering Technology (IJRASET)

spontaneous nature and lower degree of freedom of the system, respectively.

TABLE IVV
THERMODYNAMIC PARAMETERS FOR METAL ION ADSORPTION

Metal	Temperature (K)	ΔG° (cal/mol)	ΔS° (cal/mol K ⁻¹)	ΔH° (cal/mol)
Pb(II)	298.15	- 5391.38	- 29.03	7.448
	303.15	- 9760		
	308.15	-12047.1		
Zn(II)	298.15	- 3621.6	- 48.06	9.124
	303.15	- 8489.5		
	308.15	10123.42		

IV. CONCLUSIONS

Combined sol-gel and electrospinning technique appears to be a promising one for titania nanofiber synthesis. Titanium being one tested metal oxide for heavy metal was used as adsorbent in fiber form. This form provides advantage of large surface area as well as ease of handling. SEM, FTIR and BET results were promising. It can be concluded from the experimental results that titania nanofibers had good metal affinity for both Pb(II) and Zn(II) and that both followed same adsorption trend. This study showed that TNF could be used as an alternate to conventional adsorbents for the removal of metal ions from wastewater in a very short time with high removal efficiency. The removal of Pb(II) and Zn(II), as a typical metal ion commonly present in wastewaters, by adsorption onto Titania nanofibers was successfully accomplished. Adsorption was very rapid and equilibrium was achieved in about 120 min. Also adsorption was highly dependent on the initial metal ion concentration, pH and temperature. Also adsorption increased with increase in adsorbent dose and contact time, thereafter the trend varied. The adsorption isotherms were also determined and were appropriately described by both Langmuir and Freundlich models, with a better fitting to Langmuir model than Freundlich model. The thermodynamics of metal ion adsorption onto titania nanofibers confirmed the endothermic nature of the adsorption process, the spontaneity and the physisorption nature of the process. Therefore, titania nanofibers are recommended as fast and effective adsorbents for rapid removal of metal ions from wastewater effluents.

V. ACKNOWLEDGMENT

The authors acknowledge technical support from Department of Chemical Engineering, IIT (BHU), Varanasi.

REFERENCES

- [1] S. Babel and T. A. Kurniawan, "Cr(VI) removal from synthetic wastewater using coconut shell charcoal and commercial activated carbon modified with oxidizing agents and/or chitosan," *Chemosphere*, Vol. 54 (7), pp. 951-967, 2004.
- [2] J. R. Anderson and C.O. Weiss, "Method for precipitation of heavy metal sulphides," U.S. Patent 3740331, Jun. 19, 1973.
- [3] A. Smara, R. Delimi, E. Chainet and J. Sandeaux, "Removal of heavy metals from diluted mixtures by a hybrid ion-exchange/electrodialysis process," *Sep. Purif. Technol.*, Vol. 57, pp. 103-110, 2007.
- [4] I. Metcalf, Eddy, *Wastewater Engineering Treatment and Reuse*, 4th ed., McGraw Hill, New York, 2003.
- [5] W. R. Peters, E. T. White, Y. K. Carole and S. Shedroll, "Wastewater treatment-physical and chemical methods," *J. Water Pollut. Control Fed.*, Vol. 58, pp. 481-489, 1986.
- [6] J. Esalah and M. M. Husein, "Removal of heavy metals from aqueous solutions by precipitation-filtration using novel organo-phosphorus ligands," *Sep. Sci. Technol.*, Vol. 43, pp. 3461-3475, 2008.
- [7] B. A. Winfield, "The treatment of sewage effluents by reverse osmosis-pH based studies of the fouling layer and its removal," *Water Res.*, Vol. 13, pp. 561-564, 1979.
- [8] A. Afkhamia, M. S. Tehranib and H. Bagherib, "Simultaneous removal of heavy-metal ions in wastewater samples using nano-alumina modified with 2, 4-dinitrophenylhydrazine," *J. Hazard. Mater.*, Vol. 181, pp. 836-844, 2010.
- [9] J. Q. Hu, X. L. Ma, N. G. Shang, Z. Y. Xie, N. B. Wong, C. S. Lee and S. T. Lee, "Large scale rapid oxidation synthesis of SnO₂ nanoribbons," *J. Phys. Chem. B.*, Vol. 106, pp. 3823-3826, 2002.
- [10] Y. Xia, P. Yang, Y. Sun, Y. Wu, B. Mayers, B. Gates, Y. Yin, F. Kim and H. Yan, "One dimensional nanostructures: synthesis, characterization, and applications," *Adv. Mater.*, Vol. 15, pp. 353-389, 2003.
- [11] S. Luo, J. Fan, W. Liu, M. Zhang, Z. Song, C. Lin, X. Wu and P. K. Chu, "Synthesis and low-temperature photoluminescence properties of SnO₂ nanowires and nanobelts," *Nanotechnology*, Vol. 17, pp. 1695-1699, 2006.
- [12] G. N. Chaudhari, D. R. Bambole, A. B. Bodade and P. R. Padole, "Characterization of nanosized TiO₂ based H₂S gas sensor," *J. Mater. Sci.*, Vol. 41, pp. 4860-4864, 2006.
- [13] C. L. Chen and H. S. Weng, "Nanosized CeO₂-supported metal oxide catalysis for catalytic reduction of SO₂ with CO as a reducing agent," *Appl. Catal. B - Environ.*, Vol. 55, pp. 115-122, 2005.
- [14] S. J. Park, S. Bhargava, E. T. Bender, G. G. Chase and R. D. Ramsier, "Palladium nanoparticles supported by alumina nanofibers synthesized by

International Journal for Research in Applied Science & Engineering Technology (IJRASET)

electrospinning," *J. Mater. Res.*, Vol. 23, pp. 1193-1196, 2008.

[15] M. M. Demir, M. A. Gulgun, Y. Z. Menciloglu, S. S. Abramchuk, E. E. Makhaeva, A. R. Khokhlov, V. G. Matveeva and M. G. Sulman, "Palladium nanoparticles by electrospinning from Poly(acrylonitrile-co-acrylic acid)-PdCl₂ solutions: Relations between preparation conditions, particle size, and catalytic activity," *Macromolecules*, Vol. 37, pp. 1787-1792, 2004.

[16] T. Matsui, M. Harada, Y. Ichihashi, K. K. Bando, N. Matsubayashi, M. Toba and Y. Yoshimura, "Effect of noble metal particle size on the sulfur tolerance of monometallic Pd and Pt catalysts supported on high-silica USY zeolite," *Appl. Catal. A*, Vol. 286, pp. 249-257, 2005.

[17] D. Nabi, I. Aslam and I. A. Qazi, "Evaluation of the adsorption potential of titanium dioxide nanoparticles for arsenic removal," *J. Environ. Sci.*, Vol. 21, 402-408, 2009.

[18] A. J. Maira, K. L. Yeung, J. Soria, J. M. Coronado, C. Belver, C. Y. Lee and V. Augugliaro, "Gas-phase photo-oxidation of toluene using nanometer-size TiO₂ catalysts," *Appl. Catal. B-Environ.*, Vol. 29, pp. 327-336, 2001.

[19] M. Ni, M. K. H. Leung, D. Y. C. Leung and K. Sumathy, "A review and recent developments in photocatalytic water-splitting using TiO₂ for hydrogen production," *Renew. Sust. Energ. Rev.*, Vol. 11, 401-425, 2007.

[20] Z. Ding, X. Hu, G. Q. Lu, P. L. Yue, P. F. Greenfield, "Novel silica gel supported TiO₂ photocatalyst synthesized by CVD method," *Langmuir*, Vol. 16, pp. 6216-6222, 2000.

[21] P. Murugavel, M. Kalaisevam, A. R. Raju and C. N. R. Rao, "Sub-micrometre spherical particles of TiO₂, ZrO₂ and PZT by nebulized spray pyrolysis of metal-organic precursors," *J. Mater. Chem.*, Vol. 7, pp. 1433-1438, 1997.

[22] V. Tomer, R. Teye-Mensah, J. C. Tokash, N. Stojilovic, W. Kataphinan, E. A. Evans, G. G. Chase, R. D. Ramsier, D. J. Smith and D. H. Reneker, "Selective emitters for thermophotovoltaics: erbia- modified electrospun titania nanofibers," *Sol. Energy Mater. Sol. Cells*, Vol. 85, pp. 477-488, 2005.

[23] S. K. Pradhan, P. J. Reucroft, F. Yang and A. Dozier, "Growth of TiO₂ nanorods by metalorganic chemical vapor deposition," *J. Cryst. Growth*, Vol. 256, pp. 83-88, 2003.

[24] J. Yang, S. Mei and J. M. F. Ferreira, "Hydrothermal synthesis of nanosized titania powders: Influence of tetraalkyl ammonium hydroxides on particle characteristics," *J. Am. Ceram. Soc.*, Vol. 84, pp. 1696-1702, 2001.

[25] D. Li and Y. Xia, "Fabrication of Titania Nanofibers by Electrospinning," *Nano letters*, Vol. 3 (4), pp. 555-560, 2003.

[26] I. A. Zouboulis, K. N. Lazaridis and K. A. Matis, "Removal of toxic metal ions from aqueous systems by biosorptive flotation," *J. Chem. Technol. Biotechnol.*, Vol. 77, pp. 958-964, 2002.

[27] J. Eastoe and J. S. Dalton, "Dynamic surface tension and adsorption mechanisms of surfactants at the air water interface," *Adv. J. Colloid Interface Sci.*, Vol. 85, pp. 103-144, 2000.

[28] H. Freundlich, "Über die adsorption in losungen (adsorption in solution)," *Z. Phys. Chem.*, Vol. 57, pp. 384-470, 1906.

[29] A. Akgerman and M. Zardkoobi, "Adsorption of phenolic compounds on fly Ash," *J. Chem. Eng. Data*, Vol. 41, 185-187, 1996.

[30] T. Hsisheng and H. Chien-To, "Influence of Surface Characteristics on Liquid-Phase Adsorption of Phenol by Activated Carbons Prepared from Bituminous Coal," *Ind. Eng. Chem. Res.*, Vol. 39 (9), pp. 3618-3624, 1998.

[31] M. K. Mondal, "Removal of Pb(II) from aqueous solution by adsorption using activated tea waste," *Korean J. Chem. Eng.*, Vol. 27 (1), 144-151, 2010.

[32] S. Azizian, "Kinetic models of sorption: a theoretical analysis," *J. Colloid Interface Sci.*, Vol. 276 (1), pp. 47-52, 2004.

[33] L. Zhang, N. Liu, L. Yang and Q. Lin, "Sorption behavior of nano-TiO₂ for the removal of selenium ions from aqueous solution," *J. Hazard. Mater.*, Vol. 170, pp. 1197-1203, 2009.

[34] B. H. Hameed, "Evaluation of papaya seed as a non conventional low cost adsorbent for removal of MB," *J. Hazard. Mater.*, Vol. 162, 939-944, 2009.

[35] A. S. Özcan and A. Özcan, "Adsorption of acid dyes from aqueous solutions onto acid-activated bentonite," *J. Colloid Interface Sci.*, Vol. 276, pp. 39-46, 2004.

[36] G. E. Boyd, A. W. Adamson and L. S. Myers, "The exchange adsorption of ions from aqueous solutions by organic zeolites, II: kinetics," *J. Am. Chem. Soc.*, Vol. 69, pp. 2836-2848, 1947.

[37] D. Mohan and K. P. Singh, "Single- and multi-component adsorption of cadmium and zinc using activated carbon derived from bagasse-an agricultural waste," *Water Res.*, Vol. 36, pp. 2304-2318, 2002.



10.22214/IJRASET



45.98



IMPACT FACTOR:
7.129



IMPACT FACTOR:
7.429



INTERNATIONAL JOURNAL FOR RESEARCH

IN APPLIED SCIENCE & ENGINEERING TECHNOLOGY

Call : 08813907089  (24*7 Support on Whatsapp)